THE NEAR-INFRARED PERIOD-LUMINOSITY RELATIONS OF CEPHEIDS IN THE LARGE MAGELLANIC CLOUD

A Senior Scholars Thesis

by

SALMA MAHZOONI

Submitted to the Office of Undergraduate Research
Texas A&M University
in partial fulfillment of the requirements for the designation as

UNDERGRADUATE RESEARCH SCHOLAR

April 2010

Major: Physics

THE NEAR-INFRARED PERIOD-LUMINOSITY RELATIONS OF CEPHEIDS IN THE LARGE MAGELLANIC CLOUD

A Senior Scholars Thesis

by

SALMA MAHZOONI

Submitted to the Office of Undergraduate Research
Texas A&M University
in partial fulfillment of the requirements for the designation as

UNDERGRADUATE RESEARCH SCHOLAR

Approved by:

Research Advisor — Lucas Macri
Associate Dean for Undergraduate Research — Robert C. Webb

April 2010

Major: Physics

ABSTRACT

The Near-infrared Period-luminostiy Relations of Cepheids in the Large Magellanic Cloud. (April 2010)

Salma Mahzooni
Department of Physics and Astronomy
Texas A&M University

Research Advisor: Dr. Lucas Macri
Department of Physics and Astronomy

We present near-infrared (J & K_s) observations of Cepheids in the Large Magellanic Cloud. The goals of these observations are to better characterize the Cepheid Period-Luminosity relation at these wavelengths, especially for periods below 10 days, and to determine if the relation is linear or non-linear in these bandpasses.

We observed approximately 1,200 fundamental and first-overtone Cepheids originally discovered by the OGLE-II survey. We used the CTIO 1.5-m telescope and the CPAPIR camera to image 49 separate fields within the LMC in the J & K_s filters. Observations were collected from November 2006 to December 2007 and each field was imaged approximately 10 times.

The images were analyzed using standard astronomical software (IRAF and the DAOPHOT suite of photometry programs). We used the 2MASS Point Source Catalog to derive astrometric and photometric calibrations for our measurements.

We present color-magnitude diagrams (CMDs) for all fields and period-luminosity relations for the Cepheid variables. Future work will ascertain the (non)-linearity of these P-L relations and make use of our CMDs for stellar population studies.

ACKNOWLEDGMENTS

Salma Mahzooni and Lucas Macri were supported by a start-up fund at Texas A&M University.Shashi Kanbur. and Frank.Ripple. were supported by the Chretien Award from the AAS and SUNY Oswego. This work made use of the CTIO 1.5-m telescope, operated as part of the SMARTS consortium with support from the National Science Foundation through AURA, Inc.

NOMENCLATURE

CMD	Color-magnitude Diagram
LMC	Large Magellanic Cloud
NIR	Near-Infrared
PLR	Period-Luminosity Relation
PSF	Point-Spread Function

TABLE OF CONTENTS

Page

Page

LIST OF FIGURES

FIGURE Page

CHAPTER I

INTRODUCTION

Many stars in the Universe exhibit changes in their luminosity over time. We broadly refer to these stars as “variables”. The astronomers of many ancient civilizations noticed stellar variability. For example, Islamic astronomers noticed one of the brightest stars in the sky would periodically become dimmer and redder. They called this star “Algol” which means “eye of the demon”. The first European to discover a variable star was Fabricius in 1596.

Variable stars can be classified into two categories: intrinsic and extrinsic. Intrinsic variable stars are those in which the changes in brightness can be attributed to physical changes in the properties of the star such as their radius, temperature and luminosity. Among these, we can include pulsating, eruptive, and explosive variables. Extrinsic variable stars are those in which the changes in brightness are due to external factors, such as eclipses.

Stellar variability can be found among all classes of stars. In this Thesis we will focus on one particular type, called “delta Cepheid variables” or “Cepheids” for short. Cepheids are massive stars (4-12 M_{sun}) that exhibit regular pulsations with periods ranging from

---

This thesis follows the style of *The Astrophysical Journal*.

are massive stars (4-12 M_{sun}) that exhibit regular pulsations with periods ranging from ~2 to 150 days. There is a well-known correlation between the mass, period of pulsation, and average luminosity of Cepheids which has been extensively used to determine distances to other galaxies and ultimately measure the Hubble constant (H_0).

History and application of cepheid variables

As previously mentioned, the first European to discover a variable star was Fabricius in 1596. He noticed that the star omicron Ceti exhibited a sudden increase in brightness and disappeared from view two months later. We now know this is a pulsating red giant that undergoes extreme changes in brightness due to the formation of dust in its atmosphere. The sudden and extreme changes in its brightness led to its nickname of “Mira” or “miraculous”.

Nearly two centuries later, in 1784, the British amateur astronomers John Goodricke and Ed Pigott discovered several new variable stars, including β Lyrae, β Persei, and δ Cephei. δ Cephei is the prototype of an important class of variable stars which are easily recognized by their sawtooth-shaped light curves.

In 1909 Ms. Henrietta Leavitt, who was employed at the Harvard College Observatory, discovered a striking correlation between the apparent brightness and period of Cepheids in the Small Magellanic Cloud. This discovery was published three years later (Leavitt & Pickering 1912) and is shown in Figure 1. This relation is commonly called the Cepheid Period-Luminosity relation or the Leavitt Law.

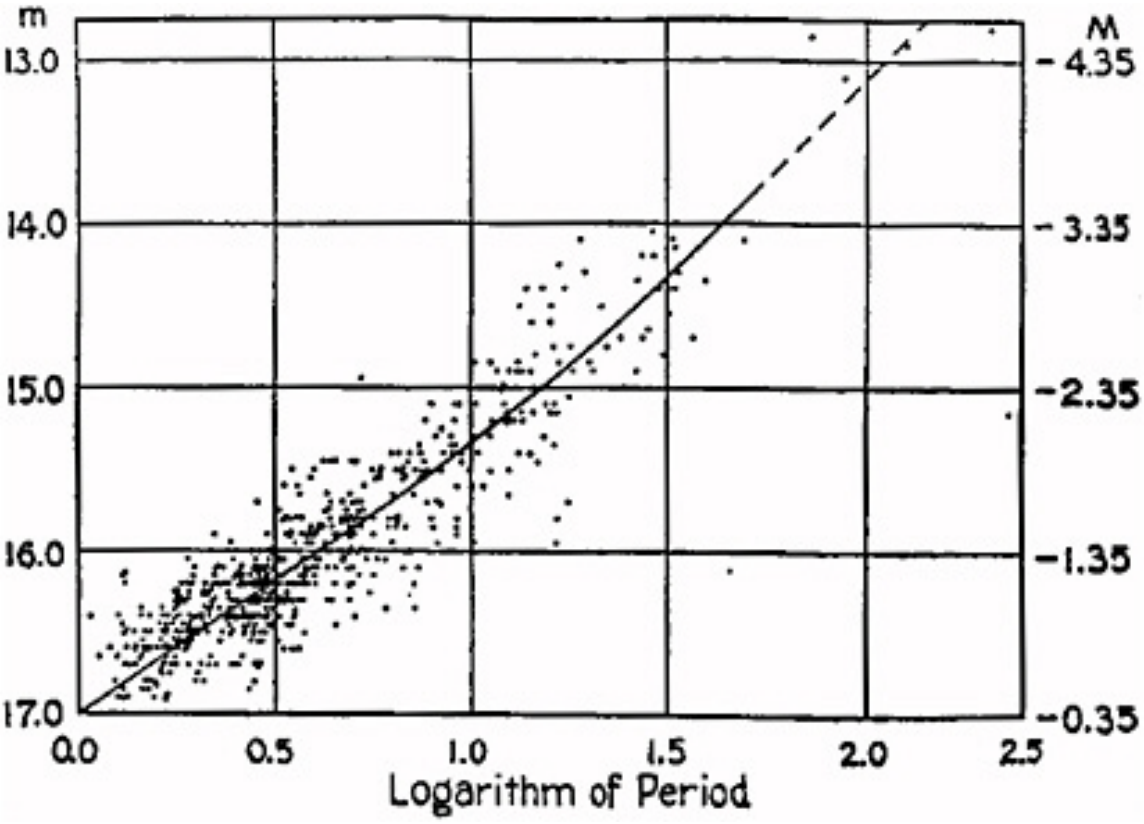

Figure 1: The original period-luminosity diagram for the Cepheids of the Small Magellanic Cloud constructed by Henrietta Leavitt in 1909. The graph illustrates the relationship between the period of a Cepheid variable and its average luminosity. m isthe apparent magnitude (left) and M is the absolute magnitude of the variable stars (right).

A decade later, Edwin Hubble discovered Cepheids in two “nebulae” (known as NGC 6822 and M33) conclusively proving their extragalactic nature and settling the decades-long debate about the existence of other galaxies in the Universe (Hubble 1925, 1926). Some of the Cepheids discovered by Hubble as part of his work can be seen in Figure 2.

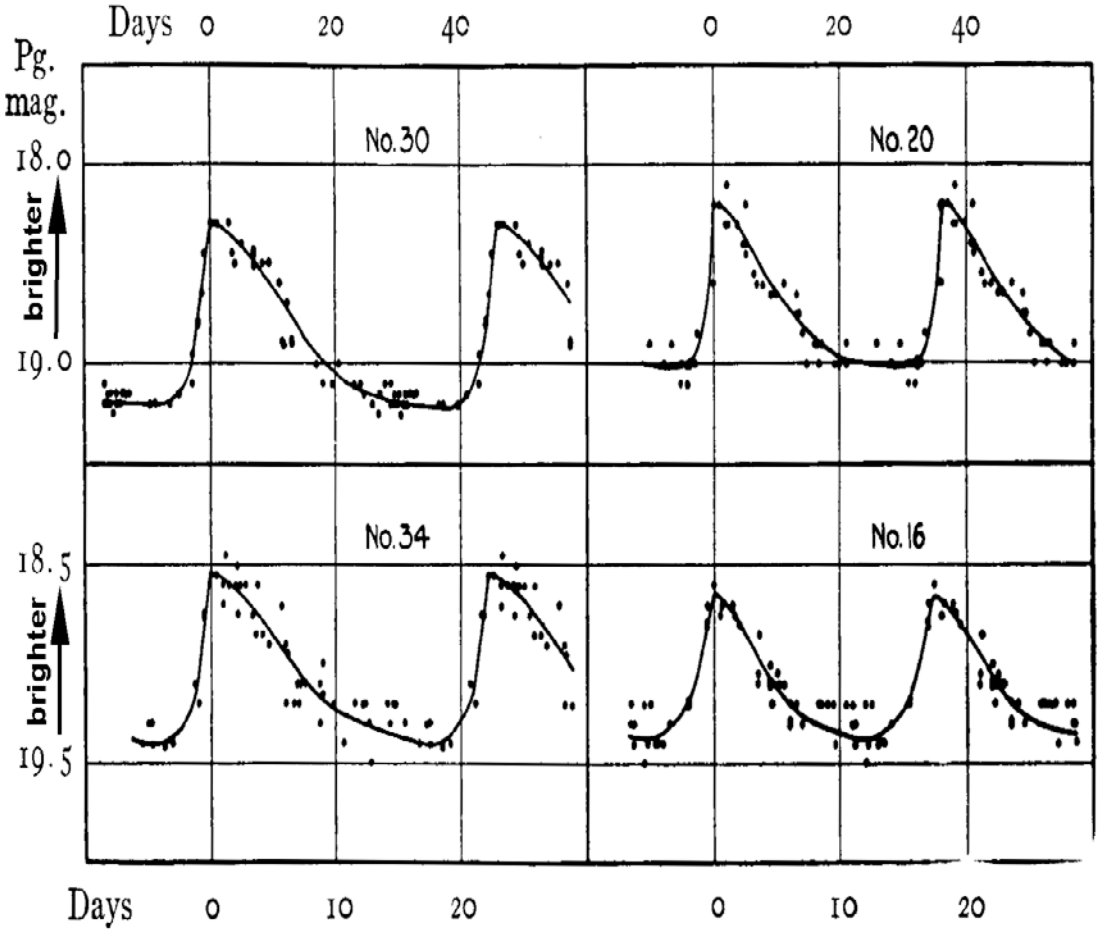

Figure 2: Light curves of Cepheid variable stars discovered by Edwin Hubble in 1925, 1926.

A few years later, Hubble used Cepheid-based distances to six galaxies in the Local Group to calibrate other techniques and determined distances to about two dozen more distant galaxies (Hubble 1929). He combined previously-published radial velocities for these galaxies with his newly-determined distances to quantify a relation between the apparent recession velocity of a galaxy (v) and its distance (d) which we now call the Hubble Law as shown in Figure 3. It is expressed as: $v = H_0 d$

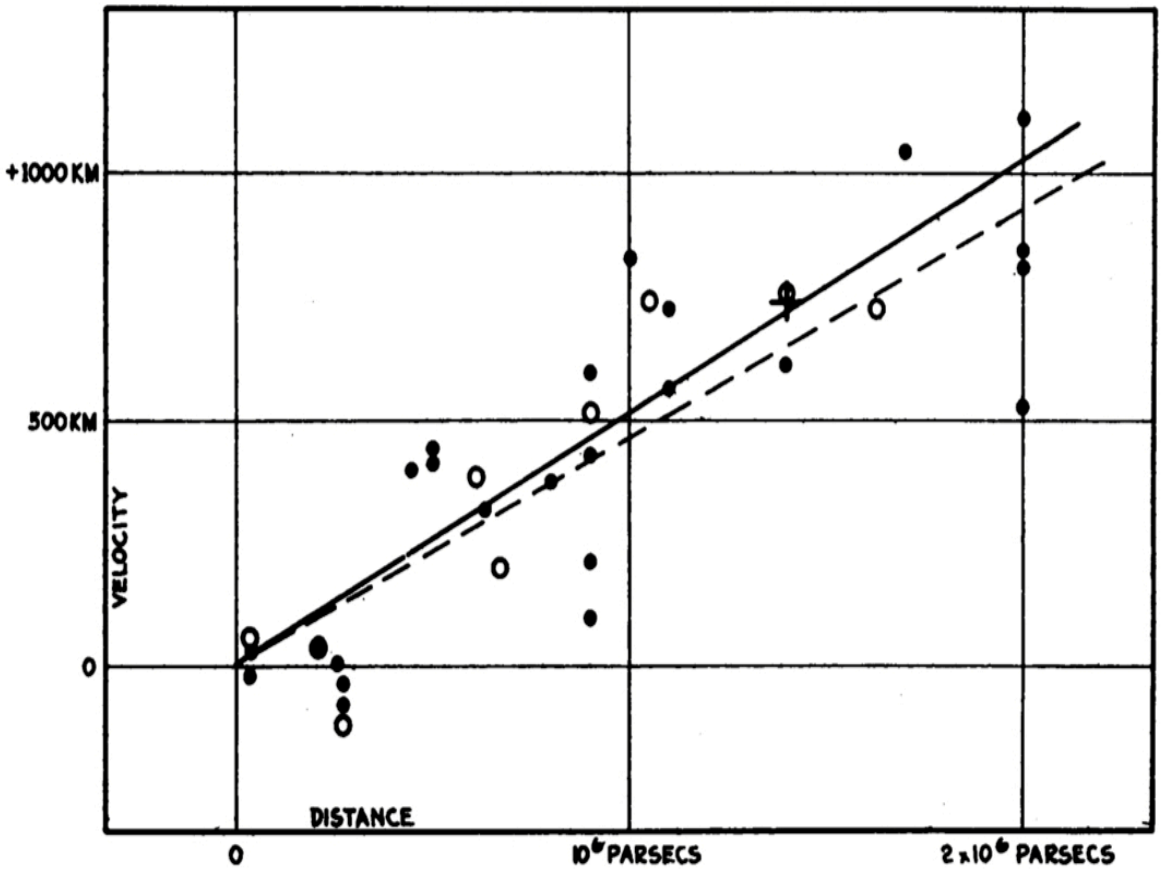

Figure 3: Plot of recession velocities versus distances derived by Edwin Hubble in 1929.

This discovery by Hubble revealed the expanding nature of our Universe. The constant of proportionality in the above equation (H_0) is called “the Hubble constant” in his honor. This constant effectively sets the cosmic distance scale for the present Universe and can also be used to determine the age of the Universe.

Improving the measurement of the Hubble constant has been a subject of vigorous work for the past 80 years. The main limitation in the measurement of H_0 is due to our inability to measure precise distances; very little error is contributed by the measurement of recession velocities. Great improvements have been made in our understanding of Cepheid variables and their P-L relations. However, we still lack a complete understanding of the pulsation mechanism behind these variables and the exact mapping of physical properties (mass, age, temperature) into observable quantities (period, luminosity). Similarly, great advancements have been made since Hubble’s original work in terms of secondary distance indicators, which are required to extend the distance scale to cosmological distances. Hubble incorrectly assumed that he could use the luminosity of the brightest stars in a galaxy as a way to venture beyond the distances to which he could discover Cepheids. Nowadays, we use several secondary distance indicators such as the Tully-Fisher relation, Type Ia supernovae and the Surface Brightness Fluctuations method. Important cross-checks of the Cepheid distances to nearby galaxies can be done using the Tip of the Red Giant Branch method. A promising

new technique involving radio observations of masers orbiting the central massive black holes of nearby galaxies can also be used to calibrate the distance scale.

The current Extragalactic Distance Scale, recently calibrated by Riess, Macri, et al. (2009) to estimate H_0 to 5% precision, has as its first rung near-infrared observations of Cepheids in the spiral galaxy NGC 4258. This galaxy is located at a distance of 7.2 Mpc (1 pc=3.3 light years) and was chosen as the first step in the scale because of its very precise and accurate maser-based distance estimate, which is uncertain only by 3% (Humphreys et al., in prep.). If one wishes to further reduce the uncertainty in H_0, additional calibrating galaxies will be required in the first rung of the scale.

The Large Magellanic Cloud (Figure 4) is a nearby (D=50 kpc) satellite galaxy of the Milky Way. It contains a large sample of Cepheid variables that are bright and well resolved. It is currently not used as another first rung in the distance scale because its distance estimate is only accurate to ~10%. However, observations in the next decade with the GAIA satellite will provide a distance measurement accurate to a few percent. Thus, the LMC will be able to contribute equally to the absolute calibration of the Cepheid Period-Luminosity relation as NGC 4258 does presently.

Figure 4: The Large Magellanic Cloud. The observations analyzed in this Thesis cover the central bar of the galaxy (outlined by the black rectangle).

Since the Large Magellanic Cloud is ~150 times closer to the Sun than NGC 4258, we can study its Cepheid variables in far greater detail. While it is rare to detect Cepheids

with periods below 10 days in other galaxies, in the case of the LMC we can discover them all the way down to the shortest periods (P~2 days).

Project overview

The aim of this Thesis is to obtain time-series near-infrared photometry of a large sample of Cepheid variables in the Large Magellanic Cloud (LMC). As described above, the Cepheid variable stars of the Magellanic Clouds have been useful tools to measure cosmic distances since Ms. Leavitt's initial discovery of the P-L relation. The goal of this Thesis is to characterize the properties of the Period-Luminosity relations at near-infrared wavelengths (1.1 & 2.2μm). This detailed characterization of the Cepheid P-L relation will increase our ability to measure Hubble constant with a greater degree of accuracy and precision.

The observations used in this Thesis were acquired using the CTIO 1.5 meter telescope and the CPAPIR camera over 33 nights between November 2006 and December 2007. The CPAPIR camera is sensitive to light between 1 and 2.5 μm and has several available filters. Our observations were carried out using three broad-band filters known as J (1.1 μm), H (1.6 μm) and K-short or K_s (2.2 μm). In this Thesis, we present the analysis of the observations taken through the J and K_s filters.

The raw images must undergo a “reduction process” which includes flat-fielding and sky subtraction. After the initial data reduction, the brightness of each star on each image is measured using the method known as Point-Spread Function (PSF) photometry. In this project, each field was imaged multiple times to recover the light curve of the variable stars. Thus, an additional step is required after the PSF photometry is completed, in order to tie all images to common photometric zero-point. Additionally, the star lists of each field were matched to previously-existing catalogs to identify the Cepheid variables in our images and to tie our photometry to the standard system. Once this step was completed, we generated light curves of the Cepheids and derived mean magnitudes for all stars in all fields. Lastly, we constructed P-L relations in two bandpasses (J & K_s) for future investigations regarding the slope, zero-point and possible non-linearity of these relations.

CHAPTER II

THEORY

This chapter will briefly review the theory behind stellar pulsation using simple models that provide an intuitive description of the pulsations.

As mentioned earlier, pulsating stars exhibit changes in luminosity, temperature and radius over time. To describe these pulsations in stars, astronomers have developed models of stellar pulsations using thermodynamics, Newton's laws, and perturbation theory. The first and simplest model is called Linear Adiabatic Theory (LAT). The second one, which is a bit more complicated, is called Linear Non-Adiabatic Theory (LNAT). The last and most complex model is known as Non-Linear Non-Adiabatic Theory (NLNAT). All three methods will be discussed, but only the derivation of the first method will be shown in this chapter.

Hydrostatic equilibrium

Before discussing pulsating stars, let us review the mechanism by which non-pulsating stars maintain a constant size. The simplest description of a star is that it is a spherical mass of plasma under hydrostatic equilibrium. This means that gravity exerts an inward force (F_g) which is exactly opposed by the pressure (F_p) exerted by the outward transport of energy generated by fusion in the core of the star. This is shown in Figure 5.

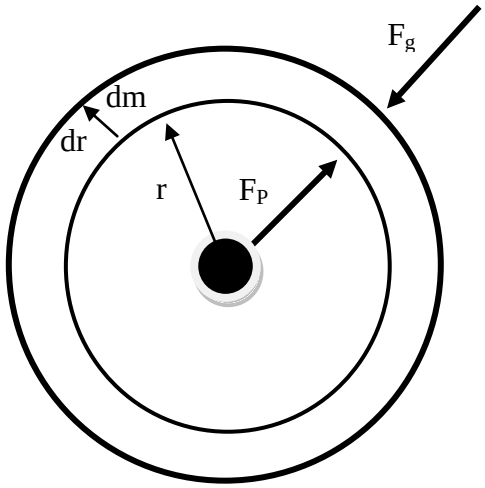

Figure 5: A force diagram of a star with mass element dm and radius dr

We can express these forces as:

$$F_p = AP \tag{2.1}$$

$$F_g = -\frac{Gmdm}{r^2} \tag{2.2}$$

where $m = \rho \int_0^r 4\pi r^2 dr dm$ and $dm = \rho A dr$. Using Newton's 2nd law, we get

$$dm\frac{d^2r}{dt^2} = \sum F = F_g - dF_P \tag{2.3}$$

where dF_p is the force of pressure difference between r and r+dr. Using equations (2.1) and (2.2), we obtain

$$\rho A dr\frac{d^2r}{dt^2} = -\frac{Gm\rho A dr}{r^2} - AdP \tag{2.4}$$

Since the star is in equilibrium, there are no accelerations and $\sum F = 0$. Then, equation (2.4) becomes

$$-\frac{Gm\rho dr}{r^2} = dP \rightarrow -\frac{Gm}{r^2}\rho = \frac{dP}{dr} = -G\frac{4}{3}\pi r\rho^2 \tag{2.5}$$

Pulsation models

There are different models to describe stellar pulsation. In the discussion below, we consider purely radial acoustic oscillations. To estimate the pulsation period, Π, we first need to know how long it would take a sound wave to propagate across the diameter of a star with radius R and constant density ρ. The adiabatic sound speed can be calculated as below.

Using the First Law of Thermodynamics for adiabatic (δQ = 0) processes, we have dU = δW, where W represents the work done by the system which depends on changes in volume and has been defined as δW = P dV.

Using the differential form of the ideal gas law P dV + V dP= n k dT and the heat capacity relation dU = C_v dT, we can calculate the speed of sound to be

$$v_{sound} = \sqrt{\frac{\gamma P}{\rho}} \tag{2.6}$$

where $\gamma \equiv \frac{C_P}{C_v}$ and ρ is density. The speed of sound depends on pressure and pressure depends on radius,

$$\frac{dP}{dr} = -\frac{4}{3}\pi\rho^2 r. \tag{2.7}$$

After integrating both sides, we get

$$P(r) = \frac{2\pi}{3} G\rho^2 (R^2 - r^2) \tag{2.8}$$

Plugging P(r) in the speed of sound equation, we arrive at:

$$v_{sound} = \sqrt{\frac{2\pi}{3}} \gamma G\rho (R^2 - r^2) \tag{2.9}$$

Now that we have calculated the velocity, we can determine the time that it takes for an adiabatic pressure wave to propagate across the diameter of the star:

$$\Pi \approx 2\int_0^R \frac{dr}{v_{sound}} = 2\int_0^R \frac{dr}{\sqrt{\frac{2\pi}{3}} \gamma G\rho (R^2 - r^2)} \tag{2.10}$$

After integrating the above, we arrive at the period-density relation which is:

$$\Pi = \sqrt{\frac{3\pi}{2\gamma G\rho}} \tag{2.11}$$

Qualitatively, this relation is confirmed by observations: the stars with the highest densities (white dwarfs) have the shortest pulsation periods.

Linear adiabatic theory

We will now describe Linear Adiabatic Theory, which was first applied to stellar pulsations by Arthur Eddington at the start of the twentieth century. In this theory, two assumptions have been made: one is that the oscillation occurs about a static point with a small amplitude, and the other is that no heat transfer takes place within different zones in the star. This method is only able to reproduce some pulsation behavior because of its limiting assumptions. However, it is able to demonstrate some important relationships between pulsation behavior and certain stellar parameters such as the famous Cepheid Period-Luminosity relation. There are many possible ways to derive this method, but the following derivation uses simple physics.

We start with Newton's second law:

$$m\frac{dv}{dt} = -\frac{GmM}{r^2} - AdP \tag{2.12}$$

where m= dm, M = mass of the star and

$$v = \frac{dr}{dt} \tag{2.13}$$

Using the adiabatic relation between pressure and volume, we get

$$P_i V_i^{\gamma} = P_f V_f^{\gamma} \tag{2.14}$$

and the volume is

$$V = \frac{4}{3}\pi r^3 \tag{2.15}$$

Thus, equation (2.8) becomes

$$P_i r_i^{3\gamma} = P_f r_f^{3\gamma} \tag{2.16}$$

The velocity can be found through the following two substitutions:

$$\frac{dv}{dt} = \frac{v_f - v_i}{\Delta t} \text{ and } \frac{dr}{dt} = \frac{r_f - r_i}{\Delta t} \tag{2.17}$$

Using equations (2.17) in equation (2.12), we obtain

$$v_f = v_i + (\frac{r_i^2 4\pi P_i}{m} - \frac{GM}{r_i^2})\Delta t \tag{2.18}$$

$$r_f = r_i + v_f \Delta t \tag{2.19}$$

Linear non-adiabatic and non-linear non-adiabatic theories

The linear non-adiabatic model assumes that energy is transferred in different parts of the star. This model enables astronomers to distinguish whether the pulsating star is stable or unstable. However, this model still makes the assumption of small amplitude oscillations. Therefore, it does not predict the final amplitude for the given mode. The most complex model is non-linear non-adiabatic theory. This method takes into account the motions and forces acting on different layers of the star.

The cepheid period-luminosity relation

The Cepheid Period-Luminosity relation was first discovered by Henrietta Leavitt in 1909. She noticed that the more luminous Cepheids in the Small Magellanic Cloud take more time go through their pulsating cycles. We can roughly derive the period-luminosity relation by starting from the period-density relation of (2.11) and making a few substitutions:

$$\Pi \propto G\rho^{-\frac{1}{2}} \propto M^{-\frac{1}{2}}R^{-\frac{3}{2}} \propto R^{-\frac{3}{2}} \propto L^{-\frac{3}{4}} \tag{2.20}$$

In the equation above, we used the relationship between density, mass and radius, as well as the Stefan-Boltzmann Law $L \propto R^2$. Astronomers usually express luminosities as "absolute magnitudes" M (not to be confussed with mass!):

$$M = -2.5 \log L + const. \tag{2.21}$$

Thus, we can rewrite (2.20) as

$$M = -2.5 \left(\frac{4}{3} \log \Pi\right) + C \approx -3.3 \log \Pi + C \tag{2.22}$$

which is outstandingly close to the actual relation obeyed by Cepheids at near-infrared wavelengths

$$M \sim -3.2 \log \Pi + C \tag{2.23}$$

CHAPTER III

METHODS

The data used in this project were collected using the CPAPIR camera at the CTIO 1.5-meter telescope between November 2006 and December 2007. Observations were made through three filters, J, H and K_s, with central wavelengths near 1.1, 1.6, and 2.2 μm, respectively. The central bar region of the Large Magellanic Cloud was covered by pointing the telescope towards 49 separate fields. Each field covered 0.5 degrees on a side, roughly the solid angle subtended by the full Moon. Observations were carried out on 33 separate nights, with each field typically imaged on 10 those nights. Every time a particular field was imaged, 6-7 short (10s) exposures were collected at slightly different positions for each filter. Approximately 18,000 individual images were collected as part of this project.

Initial data reduction

The initial data reduction was carried out using several packages that are part of the standard astronomical software known as IRAF. The goal of the initial data reduction is to remove all artifacts from a raw image so that the resulting image is an accurate record of the relative amounts of light emitted by the stars in the field of view.

Two main data reduction steps are required when dealing with near-infrared images: flat-fielding and sky subtraction. The purpose of flat-fielding is to remove the defects in an image which are caused either by the characteristics of the detector and telescope or by any dust that may be located on the filters and/or on top of the camera window. For the flat-fielding correction, one must collect a series of images of a blank, featureless, uniformly-illuminated screen or a blank area of the sky. This usually takes place during the day time (if using a featureless screen) or at sunset/sunrise (if imaging a blank part of the sky). Flat-fielding is then a simple division of each raw image by its corresponding flat field (rescaled to unity).

Sky subtraction is an important step in the data reduction process of near infrared images due to the very bright, diffuse, time-varying emission arising in the Earth's atmosphere at these wavelengths. It is important to perform an accurate sky subtraction prior to flat-fielding the raw images. Usually, alternating images of the object of interest and a nearby blank region of sky are obtained. The blank images are combined to calculate the average sky for each frame that contains the object of interest. In our case, the observations were conducted in a region with no nearby blank areas of the sky, because our fields were located within a large extended object (the LMC). Therefore, we were forced to use our science images to make sky frames. As part of our data reduction process, we made a copy of each image in which all stars were detected and masked. Every image was obtained at a slightly different position on the sky. Thus, by "dithering"

and masking stars, we were able to combine a series of images to produce a blank sky frame.

Photometry

Photometry is a technique used to measure the flux or intensity of a point source by counting the electrons collected in a Charged Coupled Device (CCD) detector. These electrons, originally created by photons incident on the detector, are linearly correlated with the apparent brightness of a star. In this project, the flux measurements were carried out using a collection of programs developed by Dr. Peter Stetson. The proper way to carry out photometry in a crowded stellar field is to use a technique known as Point Spread Function (PSF) fitting. The PSF depicts the response of an imaging system to a point object. We used bright isolated stars in each image to determine the PSF. Then we scaled this function to fit all other fainter objects. It is important to note that PSF stars may vary from image to image.

Typically, each of our 18,000 images contained 4,000 to 12,000 stellar objects, depending on the field and filter. The PSF photometry was carried out in a semi-automated manner using Tcl/Tk and Unix shell scripts that executed the DAOPHOT and ALLSTAR programs (Stetson 1987, 1994). Once photometry of each individual frame was completed, we used the (x,y) coordinates of each star determined through PSF fitting to correlate stars from one image to the next. This was done using two programs

called DAOMATCH and DAOMASTER. We then used these coordinate transformations to make a median image of the field based on the 50 individual images with best quality (small PSF, low sky) using a program called MONTAGE. Figure 6 shows median images of one of our fields in the J and K_s bands.

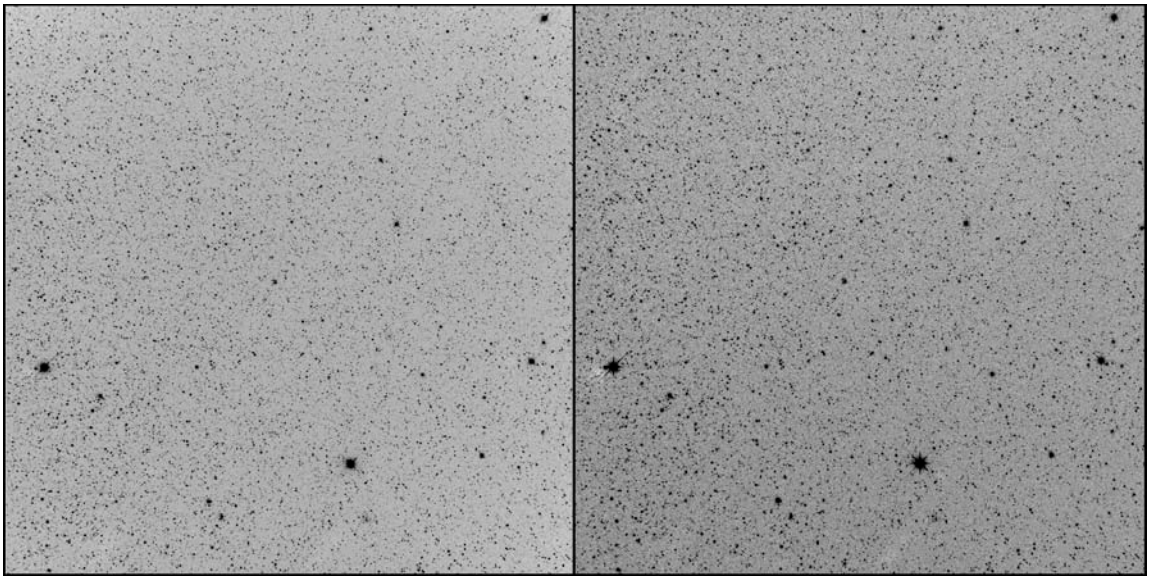

Figure 6: Median images for one of our fields in the J (left) and K_s (right) bands.

The median images were then run through PSF photometry several times using an iterative process to identify progressively fainter stars. All these stars were added to a "master list" for each field.

The next step involved measuring the magnitude of every star in the master list on each individual frame at the position predicted by the coordinate transformations previously

derived. This was carried out using a program called ALLFRAME (Stetson 1996). Next, we determined the scaling of stellar fluxes from frame to frame, since atmospheric transparency can vary from night to night. To do this we chose reference stars that satisfied several criteria: bright magnitude, low error, present in all frames as shown in Figure 7. We calculated the mean magnitudes of these stars using a program called CCDAVE and used these mean magnitudes to calculate the frame-to-frame zero-point with a program called TRIAL. This program also computes the variability of all stars and extracts the light curves of those that pass a minimum variability criterion. This appears in Figure 8. Lastly, TRIAL outputs a robust calculation of the "final" mean magnitude of all stars.

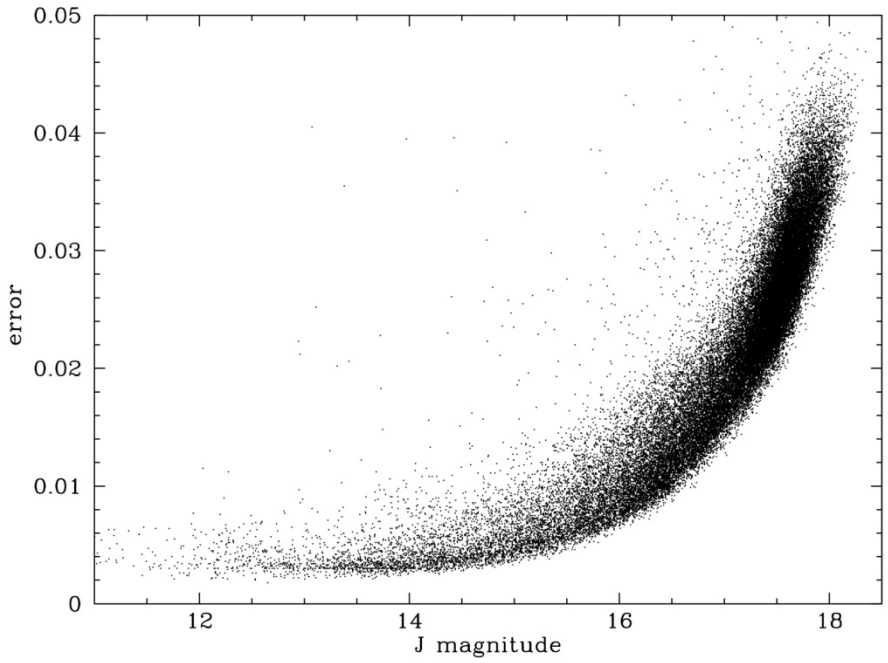

Figure 7: Measurement error versus flux (magnitude) for stars in one of our fields.

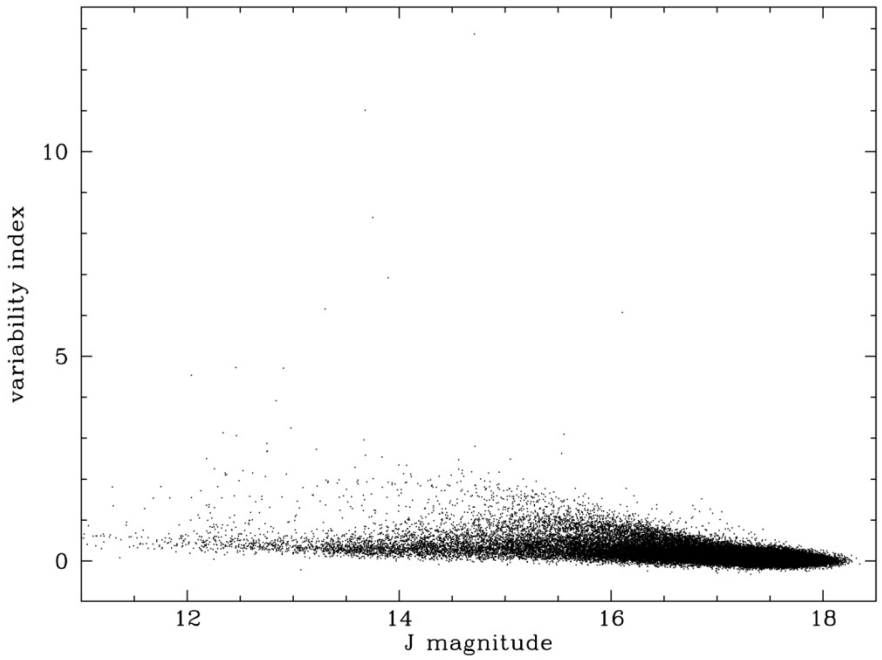

Figure 8: Variability index versus flux (magnitude) for stars in one of our fields.

Astrometric and photometric solutions

In order to identify previously-known Cepheid variables located within our fields, we must transform the arbitrary (x,y) positions of all stars into absolute coordinates referenced to the celestial sphere. This is known as the astrometric solution. We carried out this procedure by identifying stars in common between our final star lists and the

2MASS Point Source Catalog (PSC) published by Skrutskie et al. (2006). We used the IMWCS program which is part of the WCSTools package developed by Mink (2002).

The 2MASS PSC contains not only the positions but also the calibrated fluxes (or magnitudes) of bright stars located within our fields. This enabled us to determine the transformation of instrumental magnitudes into the so-called standard system. For each field and filter, we solved for an overall zero-point and a position-dependent component, modeled as a second-order polynomial. Such a position-dependent component typically arises from imperfect flat-fielding and small variations in the PSF as a function of position.

CHAPTER IV

SUMMARY AND CONCLUSIONS

After the data reduction procedures outlined in the previous chapter, we arrived at astrometrically and photometrically calibrated star lists that contain approximately 5,300,000 stars in the Large Magellanic Cloud with accurate magnitudes and variability information. We plan to use this star catalog over the next year to conduct a study of the stellar population of the LMC and all the different types of stars detected by our survey that exhibit variability.

We matched our star lists to previously published catalogs of Cepheids in the Large Magellanic Cloud by Udalski (1999) and Sebo et al. (2002) and recovered 1,165 variables. Since most of our fields have significant overlap with each other, each Cepheid was recovered multiple times for a total of 4,324 matches.

J and K_s light curves of LMC cepheids

Once the Cepheids were located in our data set, we calculated their light curves (i.e, the variation in brightness as a function of time). We phased the light curves using the periods previously determined by Udalski et al. and Sebo et al. Figure 9 shows the light

curves of six Cepheids that are representative of our entire sample. These light curves are similar to the ones shown in Figure 2 and exhibit the highly asymmetrical oscillations typical of Cepheids. For better sampled light curves, one could apply the smoothing technique known as locally regression smoother (LOESS) (Cleveland et al. 1991). However, due to the sparse sampling of our light curves, we cannot apply that technique. Instead, we must rely on template light curves to be provided by Peter Yoachim (UT Austin) in the near future. This will enable the best derivation of the mean magnitude of each Cepheid. For the remainder of this Thesis, we will use mean magnitudes calculated through a simple average of each light curve. This approach is fairly robust at near-infrared wavelengths, given the small amplitudes of pulsation.

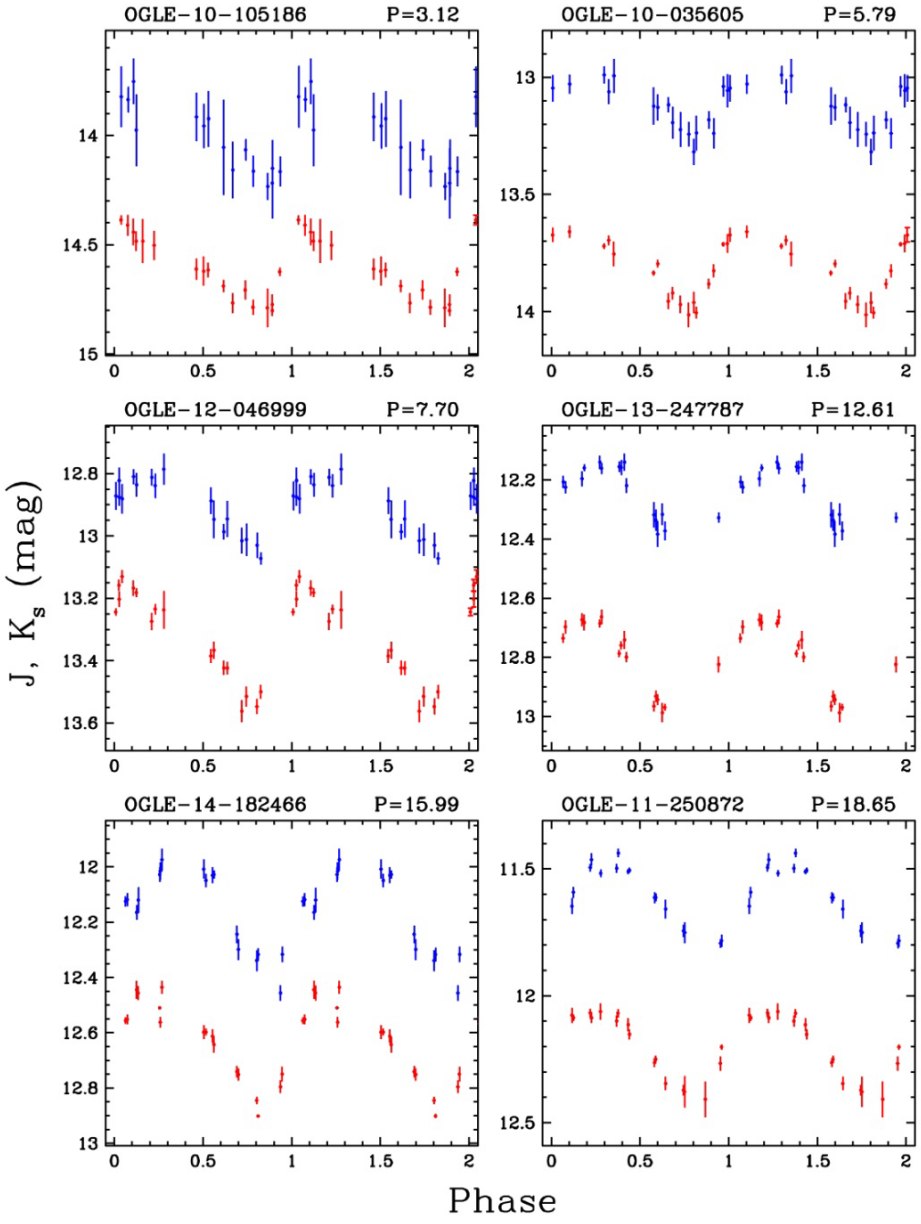

Figure 9: J- and K_s-band light curves of LMC Cepheids derived from our images. These variables were originally discovered by the OGLE-II project and have been phased using the periods derived by that survey. Two phase cycles are plotted to aid visualization of the data.

Color-magnitude diagrams

Figure 10 presents a representative color-magnitude diagram (CMD) based on our data. If we were to plot all 5,300,000 points in this figure, the density of points would render the image completely black. Thus, only about 10% of all stars are plotted. The most prominent feature in the CMD is red giant branch of LMC stars, including its tip at K~12.15 mag.

Figure 10 also contains colors and magnitudes of all Cepheids recovered in our images. They have been color-coded according to their type of pulsation, as derived by Udalski et al.: blue for overtone pulsators and red for fundamental mode pulsators. They outline two neighboring, yet separate regions of pulsation in this diagram.

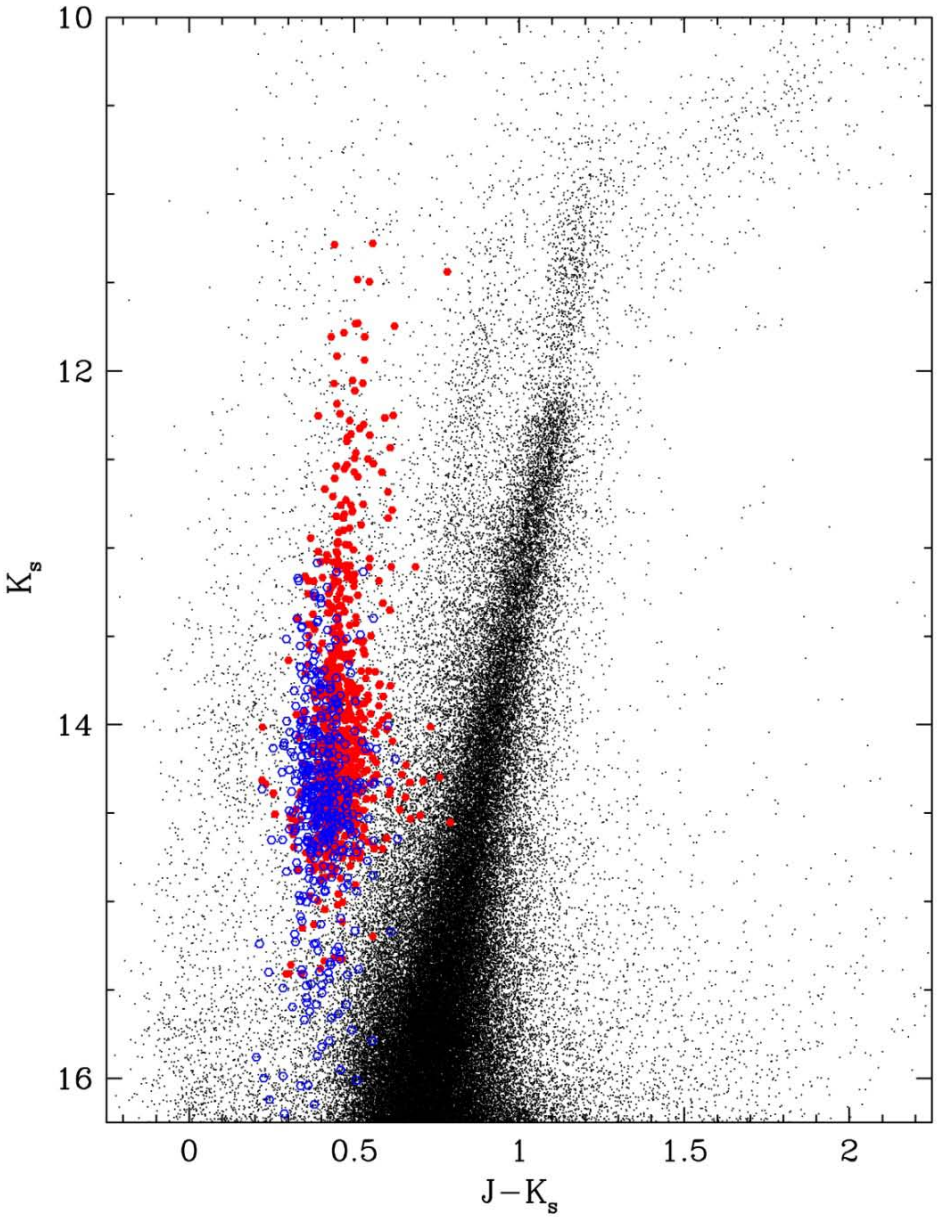

Figure 10: Color-magnitude diagram for ~10% of all stars present in our fields and for all Cepheids. The latter are plotted using blue and red symbols for overtone and fundamental mode pulsators, respectively.

Period-luminosity relations

Figure 11 presents the J and Ks period-luminosity relations for all Cepheids present in our sample. The periods were taken from their respective catalogs and the mean magnitudes were derived by the procedure described in Chapter III. Once again, the Cepheids are color-coded according to their type of pulsation (blue for overtone pulsators, red for fundamental mode pulsators).

The near-infrared Period-luminosity relations can in principle be used to determine the distance to the LMC by comparing the intercept of these relations at a fixed period to the same relations for Milky Way Cepheids, which can be calibrated into absolute magnitudes through stellar parallax measurements. Before making this calculation, one must make corrections for interstellar extinction since the amount of dust towards the LMC is not negligible. Udaslki et al. computed the extinction towards each Cepheid in the LMC by observing the variation in apparent magnitude of a feature in optical color-magnitude diagrams known as the “red clump”. Sebo et al. assumed a uniform extinction of E(B-V)=0.1 mag for their sample. We applied a correction for interstellar extinction using the appropriate values for each Cepheid.

Another application of our P-L relations will involve the search for non-linearity, or a “break” in the slope at a period of approximately 10 days. Such a break has been discovered at optical wavelengths (Kanbur & Ngeow 2004) but it is unknown at the moment whether this non-linearity extends to near-infrared wavelengths.

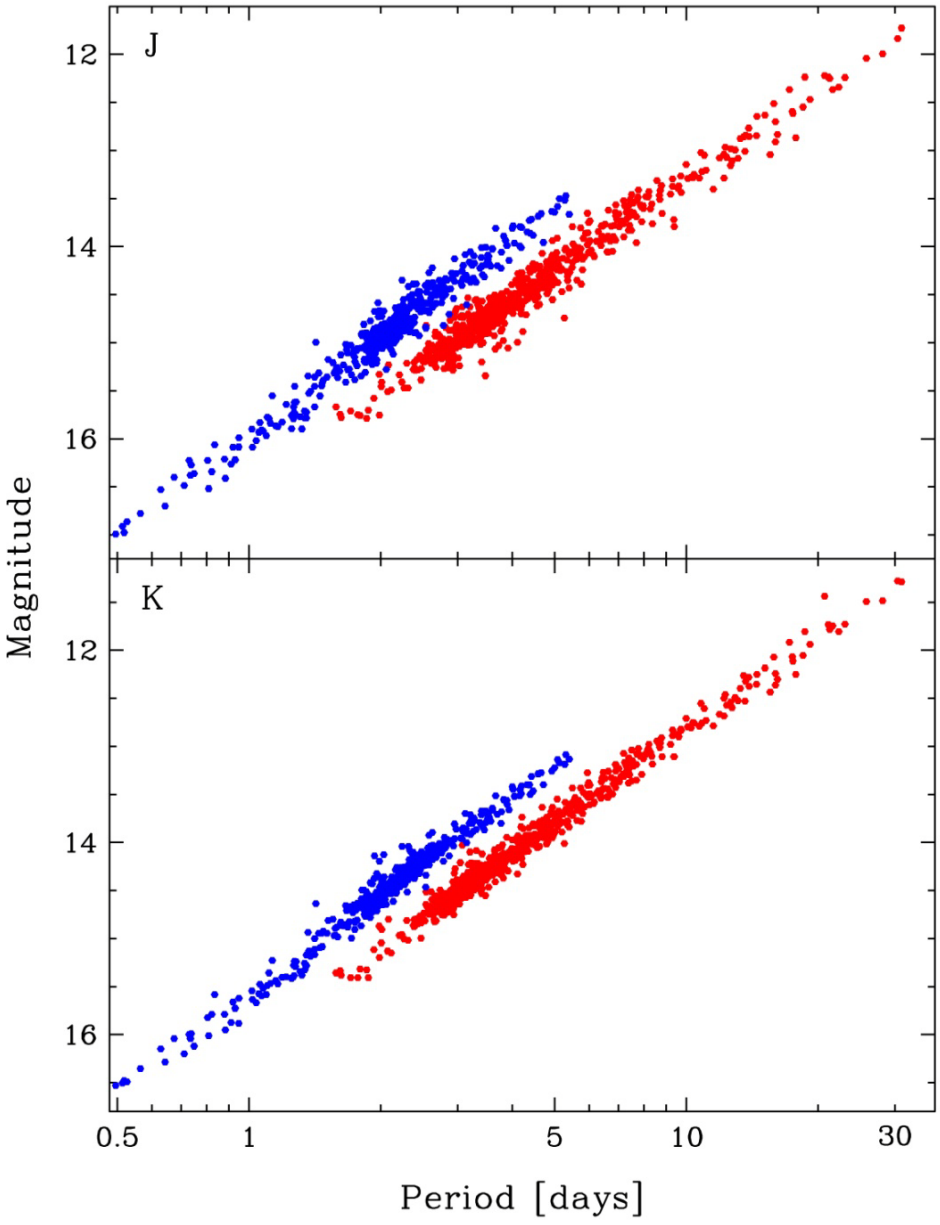

Figure 11: J and K_s Period-Luminosity relations of Cepheids in the Large Magellanic Cloud. Fundemental mode Cepheids are plotted using res symbols, while overtone pulsators are plotted using blue symbols.

Summary

We have presented J and K_s photometry for 1,165 fundamental and first-overtone Cepheids located in the Large Magellanic Cloud. This represents a ten-fold increase in the number of these variables with near-infrared data compared to the previous work of Persson et al. (2004). Additionally, we have generated accurate color-magnitude diagrams for over 5,300,000 stars which include variability information over time scales ranging from hours to over one year.

The near-infrared P-L relations have the advantage of being nearly insensitive to extinction and metallicity effects, and may also be free of non-linearities present at optical wavelengths. Future work by us and our collaborators will determine if any such non-linearity is present. Once an accurate distance to the Large Magellanic Cloud is provided by the upcoming GAIA space mission, we expect our P-L relations will be used as part of the first rung of the Extragalactic Distance Scale and future determinations of the Hubble constant.

REFERENCES

Hubble, E.1925, ApJ 62, 409

Hubble, E. 1926, ApJ 63, 236

Kanbur S.M.& Ngeow C.C.2004, MNRAS 350, 962

Leavitt, H. S., & Pickering, E. C. 1912, Harvard College Observ. Circ., 173, 1

Mink, D.2002, in Astronomical Society of the Pacific Conference Proceedings, v. 281, "Astronomical Data Analysis Software and Systems XI", Bohlender, Durand & Handley, eds, p. 169

Persson S. E., Madore B. F., Krzemin´ski W., Freedman W. L., Roth M., et al. 2004, AJ 128, 2239

Riess, A., Macri, L., Casertano, S., Sosey, M., Lampeitl, H., et al. 2009,APJ 699, 539

Sebo, K.M., Rawson, D., Mould, J., Madore, B. F., Putman, M. E., et al. 2002,ApJS 142 71

Skrutskie, M.F, Cutri, R.M., Stiening, R., Weinberg, M. D., Schneider, S. et al. 2006, AJ 131, 1163

Stetson, 1987,PASP 99, 191

Stetson, 1994, PASP 106, 250

Stetson, 1996,PASP 108, 851

Udalski, A., Pietrzynski, G. et al. 1999, Ac A, 49, 543

CONTACT INFORMATION

Name:	Salma Mahzooni
Professional Address:	Department of Physics and Astronomy 4242 TAMU Texas A&M University College Station, TX 77843
Email Address:	samahzooni@gmail.com
Education:	B.S., Physics, Texas A&M University, May 2010 Undergraduate Research Scholars